International Journal of Technology

A Novel Kinetic Model of Enzymatic Biodiesel Production in a Recirculating Fixed Bed Reactor

Frederick Soetandar[1,2,3], Ibnu Maulana Hidayatullah[1,2,4], Tania Surya Utami[1,2,4], Masafumi Yohda[3,5], Heri Hermansyah[1,2,4*]

[1]*Department of Chemical Engineering, Faculty of Engineering, Universitas Indonesia, Depok, West Java 16424, Indonesia*
[2]*Bioprocess Engineering Study Program, Faculty of Engineering, Universitas Indonesia, Depok, West Java, 16424, Indonesia*
[3]*Division of Biotechnology and Life Science, Institute of Engineering, Tokyo University of Agriculture and Technology, Koganei, Tokyo 184-8588, Japan*
[4]*Research Center for Biomass Valorization, Universitas Indonesia, Depok, West Java, 16424, Indonesia*
[5]*Institute of Global Innovation Research, Tokyo University of Agriculture and Technology, Koganei, Tokyo 184-8588, Japan*

Abstract. Entrapped lipase derived from *Candida rugosa* can be used as an alternative for commercial heterogeneous catalysts in the biodiesel synthesis process. The inclination towards a recirculating reactor with lipase-containing beds stems from its capability to simultaneously improve both yield and reproducibility in the biodiesel synthesis process. To industrialize biodiesel production with entrapped lipase in a recirculating reactor, optimization is essential, and this can be estimated using a kinetics model. In this context, a kinetics model based on the Ping-Pong Bi-Bi mechanism was developed for enzyme transesterification. Following this, experiments on biodiesel synthesis were carried out in a fixed-bed reactor with a recirculated substrate, and a biodiesel concentration of 2177.231 mol/m^3 was achieved from 917.804 mol/m^3 triglyceride. In this study, 3 models, namely Model 1, 2, and 3, were developed based on the Ping-Pong Bi-Bi mechanism, and each has assumptions that determine its complexity. To validate these models, two sets of secondary data were taken and fitted into the respective model. The sum relative error is used to express the differences between model and experimental data. Model 1, predicting each component in transesterification, exhibited the highest error of 1.64, while Model 3, assuming excess alcohol and incorporating a pseudo-steady-state for di- and monoglyceride, yielded the lowest error. Despite these variations, every model demonstrated good agreement in following each component profile accurately, providing a more precise description of the reaction elements.

1. Introduction

Homogeneous catalysts are commonly used in biodiesel production due to their relatively simpler production methodology. However, alternative approaches such as non-catalytic processes, including high-pressure methodology, acid-catalyzed esterification, and

heterogeneous catalyst transesterification has been explored (Kalita *et al.,* 2022; Feng *et al.,* 2010; Demirbas, 2008). Among these methodologies, heterogeneous catalyst transesterification is an important advancement to mitigate the well-recognized limitations associated with homogeneous catalysts and non-catalytic routes (Monika, Banga, and Pathak, 2023; Wancura *et al.,* 2021; Kareem *et al.,* 2020). The development of heterogeneous catalysts holds the potential for low-cost and stable catalysts (Aisyah *et al.,* 2023).

Nomenclature			
FAME	Fatty Acid Methyl Esters	C_i	Concentration of component i (mol m^{-3})
T	Triglyceride	k_1 to k_7	The rate constant of elementary reactions shown in Figure 4
D	Diglyceride	v_i	The reaction rate of component i (mol m^{-3}h^{-1})
M	Monoglyceride	τ	Space-time (h)
B	Biodiesel/FAME	$C_{i,est}$	Estimated concentration of i from the model (mol m^{-3})
$C_{E,tot}$	Total concentration of enzyme (kg m^{-3})	$C_{i,exp}$	Concentration of component i from empirical data (mol m^{-3})

Recent advances in heterogeneous catalyst studies present the opportunity to cost-effectively incorporate enzymes as catalysts (Kalita *et al.,* 2022; Ng *et al.,* 2022; Budžaki *et al.,* 2018). Lipase, particularly sourced from *Candida rugosa*, stands out as a recognized and effective biocatalyst for transesterification, playing a crucial role in the evolution of biodiesel production. The notable activity and ready availability of *Candida rugosa* lipase (CRL) further emphasize its efficacy in the transesterification process (Iuliano *et al.,* 2020; Yücel, Terzioğlu, and Özçimen, 2012). The use of recirculating fixed-bed reactors is preferred over other types due to their enhanced efficiency (Ani *et al.,* 2018; Ren *et al.,* 2012). These reactors not only reduce size requirements but also enable the reuse of heterogeneous catalysts compared to batch processes (Aliyah *et al.,* 2016). Despite these advantages, addressing challenges related to reaction rates, catalyst cost, and enzyme inhibition is imperative for enhancing the use of immobilized enzymes in biodiesel production (Hermansyah *et al.,* 2023; Hidayatullah *et al.,* 2018). To overcome these challenges, the application of kinetic models becomes crucial in identifying correlations among operational parameters (Hidayatullah *et al.,* 2021).

Various kinetics models have been developed to illustrate the initial rate of ester production by incorporating stepwise transesterification. These models are designed to predict reactant, by-product, and product concentrations concerning both time and substrate concentration (Rahma and Hidayat, 2023; Ezzati, Ranjbar, and Soltanabadi, 2021; Calabrò *et al.,* 2010; Pessoa, Magalhães, and Falcão, 2009; Xu, Du, and Liu, 2005). While biodiesel synthesis often involves transesterification reactions, many models simplify the process by assuming a single substrate, typically triglyceride concentration (Fedosov *et al.,* 2013; Al-Zuhair, Ling, and Jun, 2007; Al-Zuhair, 2005). Although this simplification aids in determining substrate consumption and product formation rates, it tends to overlook by-product formation. Some models use empirical equations for kinetics, lacking practicality in handling varying substrate concentrations. Intermediate products are important to be put into kinetics to fully elucidate the synthesis pathways (Muharam and Soedarsono, 2020). To address this, there is a need for a model showing stepwise biodiesel production from triglycerides, emphasizing formation sequences including enzymes.

In this study, CRL was immobilized within calcium alginate beads to serve as a biocatalyst in the reactor. A novel mathematical model was developed to predict both the reaction yield and the intermediates generated during transesterification. To illustrate changes in concentration relative to residence time, enzymatic kinetics was integrated with

plug flow mass balance. The proposed kinetics model is closely in line with experimental data, capable of representing each transesterification element (alcohol, biodiesel, triglyceride, diglyceride, monoglyceride, and glycerol), and representing enzymatic transesterification pathway following the Ping-Pong Bi-Bi mechanism. Subsequently, 3 models with different assumptions and complexity were proposed. Model 1 includes all triglyceride derivatives in the reaction and considers alcohol as the limiting reactant. Model 2 is the simplified version of model 1 by assuming pseudo-steady state for diglyceride and monoglyceride concentration. Model 3 assume excess alcohol, resulting in complete reactions and therefore assumes diglyceride and monoglyceride concentration to be zero.

2. Methods

2.1. Materials

In this study, cooking palm oil was used as a triglyceride substrate, and was produced by PT. Salim Ivomas Pratama, Tbk. (Jakarta, Indonesia). The lyophilized CRL Type VII, bovine serum albumin (BSA), and all additional reagents were purchased from Merck & Co (Rahway, NJ, USA).

2.2. Reactor configuration and design

The reactor was configured to recirculate the substate mixture with dimensions of 15 cm in length and 1.1 cm in inner diameter. Immobilized enzymes were positioned within the reactor and secured using wire mesh. To maintain a consistent temperature of 37°C, the reactor jacket was enveloped with heated water from a water bath. This setup was linked to both a peristaltic pump and a water pump. The peristaltic pump introduced the mixed substrate into the reactor while the water pump circulated heated water to ensure the reactor temperature stability.

2.3. Enzyme Immobilization

The first step of the immobilization includes the production of sodium alginate solution. Subsequently, lipase solution was introduced to a sodium alginate solution to generate a 20 ml mixture containing 1.5% sodium alginate and 100 mg of lipase. Using a syringe, the enzyme mixture was extruded into a 2% $CaCl_2$ solution. The resultant beads were left suspended in the $CaCl_2$ solution for 1 hour. Then, the beads were transferred to a fresh 2% $CaCl_2$ solution and maintained at 4°C for 24 hours.

2.4. Biodiesel Synthesis and Quantification

The substrate used for biodiesel production was palm cooking oil and methanol (>99.9%) with a total ratio of 1:3 respectively. Methanol was added stepwise onto the vessel to be pumped into the reactor. The peristaltic pump volumetric flow rate was 0.4 ml/min. After the substrate passes through the reactor, it enters the vessel to be recirculated, repeatedly. The FAME yield was evaluated using the DIN EN14103 standards, calculated according to equation 1. Biodiesel composition was analyzed with a Gas Chromatography-Flame Ionisation Detector (GC-FID) (Clarus 680, PerkinElmer®, Massachusetts, USA).

$$E = \frac{\sum(A - A_{EI})}{A_{EI}} \times \frac{W_{EI}}{W} \times 100 \qquad (1)$$

Where:

E = ester content (% w/w)
$\sum A$ = total peak area of methyl ester C6:0–C24:1
A_{EI} = peak area of internal standard C19
W_{EI} = weight of internal standard (mg)
W = weight of sample (mg).

2.5. Model mechanism and assumptions

Biodiesel synthesis was carried out in 3 sequential elementary reaction stages. The transesterification follows Ping-Pong Bi-Bi mechanism that involves the formation of diglyceride and monoglyceride, and each reaction is reversible (Bornadel *et al.,* 2013; Gog *et al.,* 2012; Fjerbaek, Christensen and Norddahl., 2009). This process was carried out involving T, A, D, B, M, and G, denoting triglyceride, alcohol, diglyceride, biodiesel, monoglyceride, and glycerol respectively. Assuming there was no water-induced hydrolysis process, the only reaction in the system is transesterification.

Each elemental reaction follows a Ping-Pong Bi-Bi mechanism with a 3-step reaction shown in Figure 1. In this model, it was assumed that substrate nor product inhibits the enzyme. The Ping-Pong Bi-Bi mechanisms were developed based on the assumption that the enzyme-fatty acid complex (EF) is irreversible after its formation. The first step in the Ping-Pong Bi-Bi transesterification mechanism is the attachment of triglycerides to the enzyme, forming an enzyme-triglyceride (ET) complex. Following this process, diglycerides are liberated, forming enzyme-diglyceride complexes (ED) and releasing monoglyceride. Enzymes will react with monoglycerides to create enzyme-monoglyceride complexes (EM). Finally, the glycerol backbone is released from the enzyme-monoglyceride complex, while the EF will react with alcohol to form biodiesel.
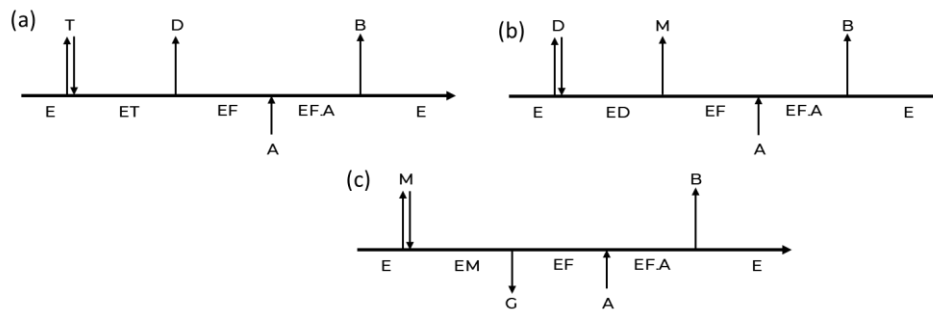
Figure 1 Concept of Ping-Pong Bi-Bi mechanism: a) triglyceride, b) diglyceride, c) monoglyceride transesterification

The mechanism of the Ping-Pong Bi-Bi transesterification was constructed using these assumptions. The mechanism itself was modified according to the method proposed by Hermansyah *et al.,* 2006. Figure 2 shows the mechanism alongside the reaction constants. The mechanism and kinetics described are designed specifically for the process of transesterification.
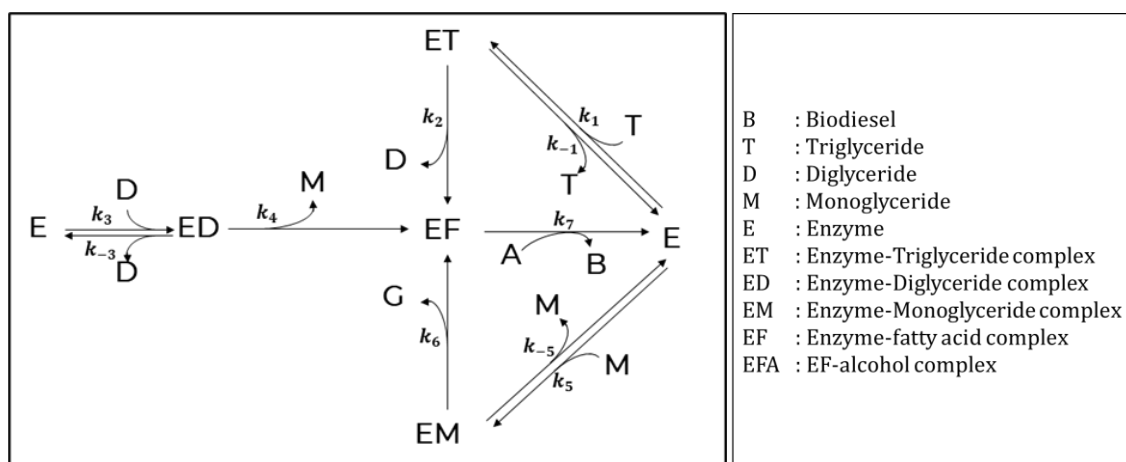
Figure 2 Mechanism of Ping-Pong Bi-Bi transesterification.

2.6. Mathematical Model Derivation

Reaction rates for the various components are written in Equation 2-7. Equation 8-11 was obtained by assuming a pseudo-steady-state for each concentration of enzyme complex compounds.

$$\frac{dC_T}{dt} = -k_1 C_E C_T - k_{-1} C_{ET} \qquad (2)$$

$$\frac{dC_{ET}}{dt} = 0 = k_1 C_E C_T - k_{-1} C_{ET} - k_2 C_{ET} \qquad (8)$$

$$\frac{dC_D}{dt} = k_2 C_{ET} - k_3 C_E C_D + k_{-3} C_{ED} \qquad (3)$$

$$\frac{dC_{ED}}{dt} = 0 = k_3 C_E C_D - k_{-3} C_{ED} - k_4 C_{ED} \qquad (9)$$

$$\frac{dC_M}{dt} = k_4 C_{ED} - k_5 C_E C_M + k_{-5} C_{EM} \qquad (4)$$

$$\frac{dC_{EM}}{dt} = 0 = k_5 C_E C_M - k_{-5} C_{EM} - k_6 C_{EM} \qquad (10)$$

$$\frac{dC_B}{dt} = k_7 C_{EF} C_A \qquad (5)$$

$$\frac{dC_{EF}}{dt} = 0 = k_2 C_{ET} - k_4 C_{ED} + k_6 C_{EM} -$$

$$\frac{dC_A}{dt} = -k_7 C_{EF} C_A \qquad (6) \qquad k_7 C_{EF} C_A \qquad (11)$$

$$\frac{dC_G}{dt} = k_6 C_{EM} \qquad (7)$$

The total concentration of the enzyme and its complex is stated in Equation 12:

$$C_{E,tot} = C_E + C_{ET} + C_{ED} + C_{EM} + C_{EF} \qquad (12)$$

Reconfiguration of equations 8-12 and substituting into Equations 2-7 yield reaction rate for each component, shown in equations 13-18. The constants in Equations 13-18 were written in Equations 19-24. These equations illustrate the forward and reverse reaction rates denoted by K_1-K_6.

$$v_T = \frac{-K_1 C_T C_{E,tot}}{1 + K_1(K_4)\frac{C_T}{C_A} + K_2(K_5)\frac{C_D}{C_A} + K_3(K_6)\frac{C_M}{C_A}} \qquad (13)$$

$$K_1 = \frac{k_1 k_2}{k_{-1} + k_2} \qquad (19)$$

$$v_D = \frac{(K_1 C_T - K_2 C_D) C_{E,tot}}{1 + K_1(K_4)\frac{C_T}{C_A} + K_2(K_5)\frac{C_D}{C_A} + K_3(K_6)\frac{C_M}{C_A}} \qquad (14)$$

$$K_2 = \frac{k_3 k_4}{k_{-3} + k_4} \qquad (20)$$

$$v_M = \frac{(K_2 C_D - K_3 C_M) C_{E,tot}}{1 + K_1(K_4)\frac{C_T}{C_A} + K_2(K_5)\frac{C_D}{C_A} + K_3(K_6)\frac{C_M}{C_A}} \qquad (15)$$

$$K_3 = \frac{k_5 k_6}{k_{-5} + k_6} \qquad (21)$$

$$v_B = \frac{C_{E,tot}(K_1 C_T + K_2 C_D + K_3 C_M)}{1 + K_1(K_4)\frac{C_T}{C_A} + K_2(K_5)\frac{C_D}{C_A} + K_3(K_6)\frac{C_M}{C_A}} \qquad (16)$$

$$K_4 = \frac{k_7 + k_2}{k_7 k_2} \qquad (22)$$

$$v_A = \frac{-C_{E,tot}(K_1 C_T + K_2 C_D + K_3 C_M)}{1 + K_1(K_4)\frac{C_T}{C_A} + K_2(K_5)\frac{C_D}{C_A} + K_3(K_6)\frac{C_M}{C_A}} \qquad (17)$$

$$K_5 = \frac{k_7 + k_4}{k_7 k_4} \qquad (23)$$

$$v_G = \frac{K_3 C_M C_{E,tot}}{1 + K_1(K_4)\frac{C_T}{C_A} + K_2(K_5)\frac{C_D}{C_A} + K_3(K_6)\frac{C_M}{C_A}} \qquad (18)$$

$$K_6 = \frac{k_7 + k_6}{k_7 k_6} \qquad (24)$$

The mass transfer in the packed bed reactor can be assumed to follow the plug flow model. The mass balance of the plug flow model is stated in Equation 25.

$$-\frac{dC_i}{d(\tau)} + v_i = 0 \qquad (25)$$

Substituting equations 13-24 into equation 25 led to these Model 1 equations, written in Equation 26-31.

$$\frac{dC_T}{d(\tau)} = \frac{-K_1 C_T C_{E,tot}}{1 + K_1(K_4)\frac{C_T}{C_A} + K_2(K_5)\frac{C_D}{C_A} + K_3(K_6)\frac{C_M}{C_A}} \qquad (26)$$

$$\frac{dC_D}{d(\tau)} = \frac{(K_1 C_T - K_2 C_D)C_{E,tot}}{1 + K_1(K_4)\frac{C_T}{C_A} + K_2(K_5)\frac{C_D}{C_A} + K_3(K_6)\frac{C_M}{C_A}} \tag{27}$$

$$\frac{dC_M}{d(\tau)} = \frac{(K_2 C_D - K_3 C_M)C_{E,tot}}{1 + K_1(K_4)\frac{C_T}{C_A} + K_2(K_5)\frac{C_D}{C_A} + K_3(K_6)\frac{C_M}{C_A}} \tag{28}$$

$$\frac{dC_B}{d(\tau)} = \frac{(K_1 C_T + K_2 C_D + K_3 C_M)\,C_{E,tot}}{1 + K_1(K_4)\frac{C_T}{C_A} + K_2(K_5)\frac{C_D}{C_A} + K_3(K_6)\frac{C_M}{C_A}} \tag{29}$$

$$\frac{dC_A}{d(\tau)} = \frac{-(K_1 C_T + K_2 C_D + K_3 C_M)C_A\,C_{E,tot}}{1 + K_1(K_4)\frac{C_T}{C_A} + K_2(K_5)\frac{C_D}{C_A} + K_3(K_6)\frac{C_M}{C_A}} \tag{30}$$

$$\frac{dC_G}{d(\tau)} = \frac{K_3 C_M C_{E,tot}}{1 + K_1(K_4)\frac{C_T}{C_A} + K_2(K_5)\frac{C_D}{C_A} + K_3(K_6)\frac{C_M}{C_A}} \tag{31}$$

Equations 26-31 can be simplified by assuming a pseudo-steady state for diglyceride and monoglyceride concentration. Therefore, Equations 13-18 can be restated as Model 2 equations, written in Equations 32-35.

$$\frac{dC_T}{d(\tau)} = \frac{-K_1 C_T C_{E,tot}}{1 + K_1(K_4)\frac{C_T}{C_A} + K_2(K_5)\frac{C_D}{C_A} + K_3(K_6)\frac{C_M}{C_A}} \tag{32}$$

$$\frac{dC_B}{d(\tau)} = \frac{(3\,K_1 C_T)C_A\,C_{E,tot}}{1 + K_1(K_4)\frac{C_T}{C_A} + K_2(K_5)\frac{C_D}{C_A} + K_3(K_6)\frac{C_M}{C_A}} \tag{33}$$

$$\frac{dC_A}{d(\tau)} = \frac{-(3\,K_1 C_T)C_A\,C_{E,tot}}{1 + K_1(K_4)\frac{C_T}{C_A} + K_2(K_5)\frac{C_D}{C_A} + K_3(K_6)\frac{C_M}{C_A}} \tag{34}$$

$$\frac{dC_G}{d(\tau)} = \frac{K_1 C_T C_{E,tot}}{1 + K_1(K_4)\frac{C_T}{C_A} + K_2(K_5)\frac{C_D}{C_A} + K_3(K_6)\frac{C_M}{C_A}} \tag{35}$$

Assuming an excess alcoholic concentration allows the elimination of the C_A term in Equations 32-35. The mathematical expressions for model 3, neglecting alcohol concentration and intermediate products, are shown in Equations 36-37.

$$\frac{dC_T}{d(\tau)} = \frac{-K_1 C_T C_{E,tot}}{1 + K_1(K_4)C_T + K_2(K_5)C_D + K_3(K_6)C_M} \tag{36}$$

$$\frac{dC_B}{d(\tau)} = \frac{3K_1 C_T C_{E,tot}}{1 + K_1(K_4)C_T + K_2(K_5)C_D + K_3(K_6)C_M} \tag{37}$$

2.7. Model Validation

The compatibility between secondary and estimation data from the developed kinetics model is shown by fitting it with transesterification data from other studies. There are 3 data sets used for model fitting, namely experimental data from this study, data from Shibasaki-Kitakawa *et al.* (2007), and data from Vicente (2006). Table 1 shows the experimental data and it was used to perform fittings with Models 2 and 3. Triglyceride and alcohol concentration in Table 1 were calculated from FAME concentration based on stoichiometric equilibrium. The data in Table S1 was obtained from Shibasaki-Kitakawa *et al.* (2007) and will be used for fitting with Model 3. The data shown in Table S2 was obtained from Vicente (2006) and will be used for fitting with Model 1. The fitting quality will be assessed using the relative error sum in Equation 38.

$$Sum\ relative\ error = \sum_{t=0}^{t=n} \left(\frac{|C_{i,est} - C_{i,exp}|}{(C_{i,est} - C_{i,exp})/2} \right)^2 \tag{38}$$

Table 1 Experimental data

| Time (h)	FAME (mol/m³)	Calculated C_T (mol/m³)	Calculated C_A (mol/m³)
0	46.964	917.804	2805.004
1	206.327	864.683	2598.677
2	361.933	812.814	2443.071
4	774.588	675.263	2030.417
8	983.446	605.643	1821.559
12	2177.231	207.715	627.7733

Using the Microsoft Excel software, differential equations were simulated through 4th-order Runge-Kutta numerical calculations, and the Solver program within Excel was used for data fitting. The alignment between experimental data and fitting results showcases the model's accuracy in estimating experimental data. Each model iteratively adjusts its kinetics parameters to minimize the sum of relative errors, aiming to achieve a value close to 0.

3. Results and Discussion

3.1. Modelling result

In Figures 3-4, Model 3 presents concentration profiles with the assumption of excess alcohol. The data fitting from Table 1 and S1 to Model 3 is shown in Figure 3a and 3b, respectively. While Model 3 is capable of estimating the formation of both biodiesel and triglycerides, it tends to overestimate the concentration of biodiesel. According to molar balance principles, it is expected that additional products arise from the transformation of triglycerides. Assuming only transesterification occurs, diglycerides and monoglycerides are expected as secondary products. However, due to Model 3 assumption of the absence of intermediate product formation, it simulates a thorough conversion of diglycerides and monoglycerides into biodiesel and glycerol.

It is crucial to take into account alcohol concentration, especially when making incremental additions, as alcohol plays the role of a limiting reactant. Model 2 incorporates alcohol concentration into its equations and assumes a pseudo-steady state for intermediates (D and M) to simplify the model. The visual representation of the fitting results obtained from the data in Table 1 can be observed in Figure 3c. Model 2 can replicate the concentration profiles of each component by assuming a pseudo-steady state for diglycerides and monoglycerides. The fitting results of Model 2 do not significantly differ from those of Model 3. This shows that Model 2 is capable of simulating the data while considering limited concentrations of methanol.
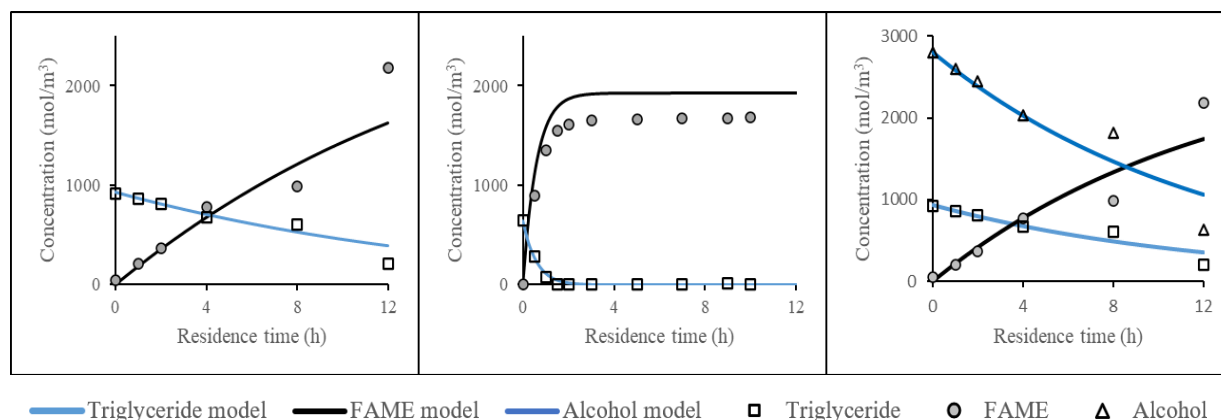
Figure 3 Fitting of a) data from this study using Model 3, b) data from Shibasaki-Kitakawa *et al.* (2007) using Model 3, and c) data from this study using Model 2

Figure 4 shows the data fitting from Table S2 into Model 1, which considers the concentration profiles of A, D, and M. The Model examines the formation of D and M as intermediates, recognizing their potential impact on biodiesel yield. Diglycerides and monoglycerides can form due to the transesterification reaction occurring in three elementary steps(Kadi *et al.,* 2019). When enzymes catalyze the formation of biodiesel, one of the three fatty acid chains on triglycerides is detached, resulting in the formation of diglycerides. Monoglycerides are generated when one of the two fatty acids in a diglyceride reacts to form biodiesel, leaving a single fatty acid chain on the glycerol molecule.

Model 1 shows a strong agreement with the data. After reaching the peak, both D and M decrease and reach very low concentrations. The reduction in the concentration of D and M is attributed to a gradual reaction with a consumption rate higher than the formation rate. The negligible amount of D and M at the higher reaction time has been observed in most reports (Chen et al., 2020; Tran, Chen and Chang, 2016; Haigh *et al.,* 2014). Model 1 can replicate this phenomenon while also simulating biodiesel formation. The model overestimates biodiesel and underestimates alcohol concentration. However, the prediction of triglyceride concentration yields accurate results. Despite triglycerides being completely consumed, the data shows a lower concentration of biodiesel than in the simulation. A few possibilities might explain this, including the potential formation of other side products such as inactive enzyme-fatty acid complexes or even the adsorption of triglycerides onto the enzyme's support matrix.
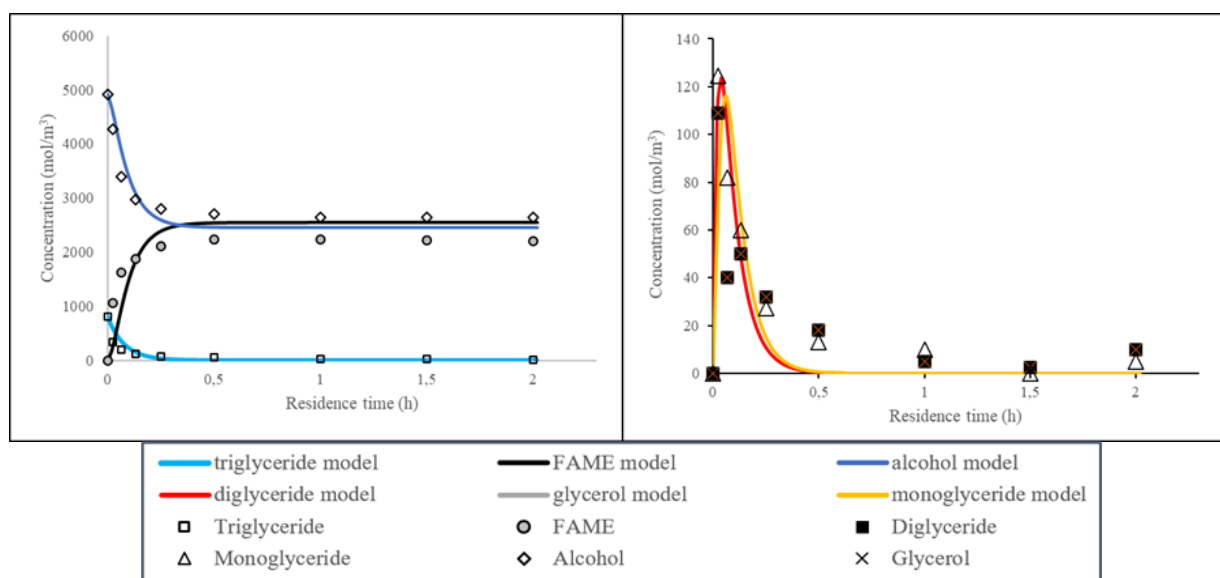
Figure 4 Fitting to Model 1 using data from Vicente *et al.* (2006)

Table 2 presents a comparison of kinetics parameters, showing the highest reaction constant derived from an experiment conducted by Vicente *et al.* (2006). The experiment used 1 wt% catalyst (based on oil) for transesterification. According to the investigation, the reactant was 240 g of *B. carinata* oil (± 800 mol/m^3), and for simplicity, it was assumed to be equivalent to 300 mL (assuming a density of 800 g/L). This led to the calculation of the concentration of catalyst used, which is 8 kg/m^3. Shibasaki-Kitakawa *et al.* (2007) synthesized biodiesel using 2 g of PA306s resin and 10g of reactants consisting of oil and 10 - 20 molar equivalents of methanol (based on oil). Assuming this 10g was equal to 20 ml of reactant, the concentration of the catalyst is estimated to be 100 kg/m^3. Although the kinetics constant for each catalyst might appear low, the overall reaction rate can be substantial with the assistance of a significant quantity of catalysts.

Table 2 Comparison of kinetics parameter

Kinetics constant	Model 1	Model 3		Model 2
	Data from:			
	Vicente *et al.* (2006)	Shibasaki-Kitakawa *et al.* (2007)	This study	This study
K_1	1.59	9.95×10^{-2}	1.70×10^{-1}	4.58×10^{-2}
K_2	6.55	-	-	-
K_3	6.27	-	-	-
K_4	0	2.77×10^{-6}	8.00×10^{-5}	6.66×10^{-3}
K_5	6.09	2.60×10^{-6}	8.28×10^{-3}	4.55×10^{-3}
K_6	8.40	2.70×10^{-6}	8.28×10^{-3}	5.47×10^{-2}
$C_{E,tot}$	8	100	1.77	1.77
sum relative error	1.64	3.49×10^{-2}	4.13×10^{-2}	5.05×10^{-2}

In the context of the stepwise transesterification reaction, K_1 signifies the inclination to yield diglycerides. K_2 represents the tendency to generate monoglycerides from diglycerides, and K_3 shows the propensity to release glycerol from monoglycerides. These constants show forward reactions. In Models 2 and 1, where diglycerides and monoglycerides are assumed to react rapidly, K_2 and K_3 are excluded. Conversely, K_4, K_5, and K_6 denote hindrances to biodiesel formation. K_4-K_6 are associated with k_2, k_4, and k_6, reflecting the rate constants of diglyceride, monoglyceride, and glycerol release. K_4 represents the dissociation of triglyceride, leading to the enzyme complex producing biodiesel from the fatty acid of triglyceride. The same meaning also applies to K_5 and K_6, with the only difference in the source of fatty acid (such as diglyceride for K_5, and monoglyceride for K_6).

In Model 3, a total of 6 parameters need to be estimated, while Models 1 and 2 require 4. The resulting parameter data shows that ion exchange resin exhibits the highest K_1 reaction rate. Model 2, assuming a controlled alcohol reaction, shows significant changes in the constant K_6 when compared to Model 1. The experiment carried out by Vicente et al. (2006) had the highest value of kinetics constants compared to other studies.

4. Conclusions

In conclusion, 3 mechanistic models based on the Ping-Pong Bi-Bi mechanism were developed to predict how each part of triglyceride transesterification behaves. Each model could provide a better understanding of how both the reactants and products change over time. Model key parameter helps to explain how operational conditions affect the transesterification process. Data fitting of this experiment data into Model 3 resulted in 4.13×10^{-2}, which shows good alignment. However, Model 1 had a high sum relative error, due to many substrates and product concentrations that the model need to adjust, therefore the sum relative error calculates all the misalignments, producing the highest sum of error. This model could become a go-to reference for understanding transesterification kinetics and further studies on the inhibition of substrate and product are needed to improve the model.

Acknowledgments

References

Aisyah, A.N., Ni'maturrohmah, D., Putra, R., Ichsan, S., Kadja, G.T.M, Lestari, W.W., 2023. Nickel Supported on MIL-96(Al) as an Efficient Catalyst for Biodiesel and Green Diesel Production from Crude Palm Oil. *International Journal of Technology,* Volume 14(2), pp. 276–289

Aliyah, A.N., Edelweiss, E.D., Sahlan, M., Wijanarko, A., Hermansyah, H., 2016. Solid State Fermentation Using Agroindustrial Wastes To. *International Journal of Technology*, Volume 8, p.1392–1403

Al-Zuhair, S., 2005. Production of Biodiesel By Lipase-Catalyzed Transesterification of Vegetable Oils: A Kinetics Study. *Biotechnology Progress*, Volume 21(5), pp. 1442–1448

Al-Zuhair, S., Ling, F.W., Jun, L.S., 2007. Proposed Kinetic Mechanism Of The Production Of Biodiesel From Palm Oil Using Lipase. *Process Biochemistry*, Volume 42(6), pp. 951–960

Ani, F.N., Said, N.H., Said, M.F.M., 2018. Optimization of Biodiesel Production using a Stirred Packed-bed Reactor. *International Journal of Technology,* Volume 9(2), pp. 219–228

Bornadel, A., Åkerman, C.O., Adlercreutz, P., Hatti-Kaul, R., Borg, N., 2013. Kinetic Modeling of Lipase-Catalyzed Esterification Reaction Between Oleic Acid and Trimethylolpropane: A Simplified Model for Multi-Substrate Multi-Product Ping–Pong Mechanisms. *Biotechnology Progress*, Volume 29(6), pp. 1422–1429

Budžaki, S. Miljić, G., Sundaram, S., Tišma, M., Hessel, V., 2018. Cost Analysis of Enzymatic Biodiesel Production in Small-Scaled Packed-Bed Reactors. *Applied Energy*, Volume 210(6), pp. 268–278

Calabrò, V., Ricca, E., De Paola, M.G., Curcio, S., Iorio, G., 2010. Kinetics of Enzymatic Trans-Esterification of Glycerides For Biodiesel Production. *Bioprocess and Biosystems Engineering*, Volume 33(6), pp. 701–710

Chen, X., Li, Z., Chun, Y., Yang, F., Xu, H., Wu, X., 2020. Effect of the Formation of Diglyceride/Monoglycerides on the Kinetic Curve in Oil Transesterification with Methanol Catalyzed by Calcium Oxide. *ACS Omega*, Volume 5(9), pp. 4646-4656

Demirbas, A., 2008. Biodiesel: A Realistic Fuel Alternative For Diesel Engines. In: *Biodiesel: A Realistic Fuel Alternative for Diesel Engines*. London: Springer

Ezzati, R., Ranjbar, S., Soltanabadi, A., 2021. Kinetics Models Of Transesterification Reaction For Biodiesel Production: A Theoretical Analysis. *Renewable Energy*, Volume 168, pp. 280–296

Fedosov, S.N., Brask, J., Pedersen, A.K., Nordblad, M., Woodley, J.M., Xu, X., 2013. Kinetic Model Of Biodiesel Production Using Immobilized Lipase Candida Antarctica Lipase B. *Journal of Molecular Catalysis B: Enzymatic*, Volume 85, pp. 156–168

Feng, Y., He, B., Cao, Y., Li, J., Liu, M., Yan, F., Liang, X., 2010. Biodiesel Production Using Cation-Exchange Resin as Heterogeneous Catalyst. *Bioresource Technology*, Volume 101(5), pp. 1518–1521

Fjerbaek, L., Christensen, K., Norddahl, B., 2009. A Review of The Current State of Biodiesel Production Using Enzymatic Transesterification. *Biotechnology and Bioengineering,* Volume 102(5), pp. 1298–1315

Gog, A., Roman, M., Toşa, M., Paizs, C., Irimie, F., 2012. Biodiesel Production using Enzymatic Transesterification – Current State and Perspectives. *Renewable Energy,* Volume 39(1), pp. 10–16

Haigh, K., Vladisavljević, G.T., Reynolds, J.C., Nagy, Z., Saha, B., 2014. Kinetics of the Pre-treatment of Used Cooking Oil using Novozyme 435 for Biodiesel Production. *Chemical Engineering Research and Design*, Volume 92(4), pp. 713–719

Hermansyah, H., Ibnu-Maulana, H., Frederick, S., Pingkan-Vanessa, S., Patrick, C., 2023. Ion Exchange Resin and Entrapped *Candida rugosa* Lipase for Biodiesel Synthesis in the

Recirculating Packed-Bed Reactor : A Performance Comparison of Heterogeneous Catalysts. *Energies*, Volume 16(12), p. 4765

Hermansyah, H., Kubo, M., Shibasaki-Kitakawa, N., Yonemoto, T., 2006. The Mathematical Model For Stepwise Hydrolysis Of Triolein Using *Candida Rugosa* Lipase In A Biphasic Oil-Water System. *Biochemical Engineering Journal*, Volume 31(2), pp. 125–132

Hidayatullah, I.M., Arbianti, R., Utami, T.S., Suci, M., Sahlan, M., Wijanarko, A., Gozan, M., Hermansyah, H., 2018. Techno-Economic Analysis Of Lipase Enzyme Production From Agro-Industry Waste With Solid State Fermentation Method. *IOP Conference Series: Materials Science and Engineering*, Volume 316(1), p. 012064

Hidayatullah, I.M., Makertihartha, I.G.B.N., Setiadi, T., Kresnowati, M.T.A.P., 2021. Modeling-Based Analysis And Optimization Of Simultaneous Saccharification and Fermentation For The Production Of Lignocellulosic-Based Xylitol. *Bulletin of Chemical Reaction Engineering & Catalysis*, Volume 16(4), pp. 857–868

Iuliano, M., Sarno, M., De Pasquale, S., Ponticorvo, E., 2020. Candida rugosa lipase for the biodiesel production from renewable sources. *Renewable Energy*, Volume 162, pp. 124-133

Kadi, M., Akkouche, N., Awad, S., Loubar, K., Tazerout, M., 2019. Kinetic Study of Transesterification Using Particle Swarm Optimization Method. *Heliyon*, Volume 5(8), p. 101016

Kalita, P., Basumatary, B., Saikia, P., Das, B., Basumatary, S., 2022. Biodiesel As Renewable Biofuel Produced Via Enzyme-Based Catalyzed Transesterification. *Energy Nexus*, Voume 6, p. 100087

Kareem, S.O., Falokun, E.I., Balogun, S.A., Akinloye, O. A., Omeike, S.O., 2020. Improved Biodiesel From Palm Oil Using Lipase Immobilized Calcium Alginate And Irvingia Gabonensis Matrices. *Beni-Suef University Journal of Basic and Applied Sciences*, Volume 9(1), p. 101186

Monika, Banga, S., Pathak, V.V., 2023. Biodiesel production from waste cooking oil: A comprehensive review on the application of heterogenous catalysts. *Energy Nexus*, Volume 10(5), p. 100209.

Muharam, Y., Soedarsono, J.A. 2020. Hydrodeoxygenation of Vegetable Oil in a Trickle Bed Reactor for Renewable Diesel Production. *International Journal of Technology*, Volume 11(7), pp. 1292–1299

Ng, W.Z., Obon, A.A., Lee, C.L., Ong, Y.H., Gourich, W., Maran, K., Tang, D.B.Y., Song, C.P., Chan, E.S., 2022. Techno-Economic Analysis Of Enzymatic Biodiesel Co-Produced In Palm Oil Mills From Sludge Palm Oil For Improving Renewable Energy Access In Rural Areas. *Energy*, Volume 243, p. 122745

Pessoa, F.L.P., Magalhães, S.P., Falcão, P.W.C., 2009. Kinetic Study of Biodiesel Production by Enzymatic Transesterification of Vegetable Oils. *Computer Aided Chemical Engineering,* Volume 27, pp. 1809-1814

Rahma, F.N., Hidayat, A., 2023. Biodiesel Production from Free Fatty Acid using ZrO2/Bagasse Fly Ash Catalyst. *International Journal of Technology*, Volume 14(1), pp. 206–218

Ren, Y., He, B., Yan, F., Wang, H., Cheng, Y., Lin, L., Feng, Y., Li, J., 2012. Continuous Biodiesel Production in a Fixed Bed Reactor Packed with Anion-Exchange Resin as Heterogeneous Catalyst. *Bioresource Technology*, Volume 113, pp. 19–22

Shibasaki-kitakawa, N., Honda, H., Kuribayashi, H., Toda, T., 2007. Biodiesel Production Using Anionic Ion-Exchange Resin As A Heterogeneous Catalyst. *Bioresource Technology,* Volume 98(2), pp. 416–421

Tran, D.T., Chen, C.L., Chang, J.S., 2016. Continuous Biodiesel Conversion via Enzymatic

Transesterification Catalyzed By Immobilized Burkholderia Lipase in a Packed-Bed Bioreactor. *Applied Energy*, Volume 168, pp.340-350

Vicente, G., Martínez, M., Aracil, J., 2006. Kinetics Of Brassica Carinata Oil Methanolysis. *Energy and Fuels*, Volume 20(4), pp. 1722–1726

Wancura, J.H., Fantinel, A.L., Ugalde, G.A., Donato, F.F., De Oliveira, J.V., Tres, M.V., Jahn, S.L., 2021. Semi-Continuous Production of Biodiesel on Pilot Scale via Enzymatic Hydroesterification of Waste Material: Process and Economics Considerations. *Journal of Cleaner Production*, Volume 285, p. 124838

Xu, Y., Du, W., Liu, D., 2005. Study On The Kinetics of Enzymatic Interesterification Of Triglycerides For Biodiesel Production With Methyl Acetate As The Acyl Acceptor. *Journal of Molecular Catalysis B: Enzymatic*, Volume 32(5–6), pp. 241–245

Yücel, S., Terzioğlu, P., Özçimen, D., 2012. Lipase Applications in Biodiesel Production. In *Biodiesel: Feedstocks, Production and Applications.* IntechOpen